High Spin-Flip Efficiency at 255 GeV for Polarized Protons in a Ring With Two Full Siberian Snakes

H. Huang, J. Kewisch, C. Liu, A. Marusic, W. Meng, F. Méot, P. Oddo, V. Ptitsyn, V. Ranjbar, and T. Roser
Brookhaven National Laboratory, Upton, New York 11973, USA

(Received 24 January 2018; published 28 June 2018)

In polarized proton collision experiments, it is highly advantageous to flip the spin of each bunch of protons during the stores to reduce the systematic errors. Experiments done at energies less than 2 GeV have demonstrated a spin-flip efficiency over 99%. At high energy colliders with Siberian snakes, a single magnet spin flipper does not work because of the large spin tune spread and the generation of multiple, overlapping resonances. A more sophisticated spin flipper, constructed of nine-dipole magnets, was used to flip the spin in the BNL Relativistic Heavy Ion Collider. A special optics choice was also used to make the spin tune spread very small. A 97% spin-flip efficiency was measured at both 24 and 255 GeV. These results show that efficient spin flipping can be achieved at high energies using a nine-magnet spin flipper.

DOI: 10.1103/PhysRevLett.120.264804

Introduction.—Experiments of polarized proton collisions in the BNL Relativistic Heavy Ion Collider (RHIC) [1], as well as a future polarized electron ion collider [2], need to measure the spin effect at the level of 10^{-3} to 10^{-4}. For such high precision measurements, frequent polarization sign reversal is imperative to avoid systematic errors from the bunch spin pattern. A spin flipper in each ring is needed which is capable of reversing the polarization sign of all bunches without changing other beam parameters.

To avoid polarization loss during acceleration and at store, high energy polarized proton colliders require full Siberian snakes, which are specially arranged magnets to rotate the spin around an axis in the horizontal plane by 180° [3]. For the RHIC, a pair of Siberian snakes is installed in each ring. The two Siberian snakes are located in the opposite side of the ring (or separated by 180°), with their spin precession axes differing by 90°. This configuration yields a spin tune ν_s as $\frac{1}{2}$ [1], where the spin tune ν_s, defined as the number of spin precessions per turn, is given by $\nu_s = G\gamma$ in the absence of Siberian snakes (γ is the Lorentz factor, G is the gyromagnetic anomaly, and $G = 1.7928$ for the protons) [4]. The traditional spin flipping technique uses a single rf spin rotator that rotates the spin around an axis in the horizontal plane. The spin rotator can be implemented as a rf dipole or a rf solenoid. Experiments done at low energies (from 100 MeV to 2 GeV) have demonstrated a spin-flip efficiency of more than 99% [5–8]. The spin flip is achieved by ramping the rf spin rotator tune $\nu_{\rm osc}$ across the spin tune ν_s adiabatically. It should be noted that such a single spin rotator generates two spin resonances, one at $\nu_s = \nu_{\rm osc}$ and one at $\nu_s = 1 - \nu_{\rm osc}$, or the so-called mirror resonance. As long as the spin tune is sufficiently far from the half integer—say, at 0.47—then the two spin resonances are sufficiently far from each other and each one can be treated as an isolated resonance. This is the case for low energies when Siberian snakes are not needed and the spin tune is not at or near the half integer. In high energy polarized proton colliders such as the RHIC, the spin tune is very close to the half integer. The two spin resonances overlap, and their interference makes full spin flip impossible with such a single rf spin rotator. To reach full spin flip, the mirror resonance has to be eliminated [9].

Spin flipper configuration.—For the spin flipper to work with a spin tune near 0.5, it has to induce only one spin resonance at $\nu_s = \nu_{\rm osc}$. In addition, it is critical to eliminate any global vertical betatron oscillations driven by the ac dipole to achieve full spin flip [10]. Thus, we have chosen a spin flipper design which consists of five ac dipoles with a horizontal magnetic field and four dc dipoles with a vertical magnetic field, which not only eliminates the mirror resonance but also forms two closed vertical orbital bumps and eliminates the global vertical oscillations outside the spin flipper [11]. Figure 1 shows the schematic drawing of the spin flipper design. The first three ac dipoles form the first closed orbital bump and the last three ac dipoles form the second closed orbital bump. The middle ac dipole (no. 3) is used twice. The four dc dipoles yield spin rotation angles of $+\psi_0/-\psi_0/-\psi_0/+\psi_0$. The rotation angle ψ_0 is given by

$$\psi_0 = (1 + G\gamma)\frac{B_{\rm dc}L}{B\rho}, \tag{1}$$

where $B\rho$ is the beam particle magnetic rigidity and $B_{\rm dc}L$ is the integrated B field of each dc dipole. These dc dipoles create a closed local horizontal bump and leave the spin tune ν_s unchanged. The five ac dipoles are operated at a frequency of about half of the revolution frequency so that

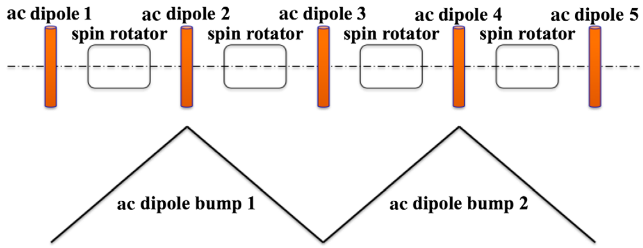

FIG. 1. The schematics of the proposed high energy spin flipper. It consists of five ac dipoles and four dc dipoles.

the tune $\nu_{\rm osc}$ is in the vicinity of ν_s. ac dipoles 1–3 and ac dipoles 3–5 create a local vertical orbit bump with a $+\phi_{\rm osc}/-2\phi_{\rm osc}/+\phi_{\rm osc}$ spin rotation sequence. The rotation angle $\phi_{\rm osc}$ is given by

$$\phi_{\rm osc} = (1+G\gamma)\frac{B_{\rm ac}l}{B\rho}, \tag{2}$$

where $B_{\rm ac}l$ is the integrated B field of the ac dipole. This configuration induces a spin resonance at $\nu_{\rm osc} = \nu_s$ while eliminating the mirror resonance at $1-\nu_s$, therefore ensuring a single resonance crossing during a $\nu_{\rm osc}$ sweep through $\nu_s \approx \frac{1}{2}$ and producing full spin flip. In the presence of a mirror resonance, the isolated resonance crossing condition would otherwise require ν_s to be far enough away from $\frac{1}{2}$. The effective spin resonance strength of the spin flipper ϵ_k then becomes

$$\epsilon_k = 2\frac{\phi_{\rm osc}}{\pi}\sin\psi_0 \sin\frac{\psi_0}{2}. \tag{3}$$

In order to eliminate the global ac dipole driven vertical betatron oscillations, the currents of the five ac dipoles have to satisfy Eq. (4) so that they excite only two closed vertical orbit bumps:

$$\begin{aligned}
I_2 &= I_0\sin(2\pi\nu_{\rm osc}i+\chi_1),\\
I_4 &= I_0\sin(2\pi\nu_{\rm osc}i+\chi_2),\\
I_1 &= \frac{1}{2}I_0\sin(2\pi\nu_{\rm osc}i+\chi_1+\pi),\\
I_5 &= \frac{1}{2}I_0\sin(2\pi\nu_{\rm osc}i+\chi_2+\pi),\\
I_3 &= I_1 + I_5,
\end{aligned} \tag{4}$$

where I_k is the current of the kth ac dipole and i is the ith orbital revolution. χ_1 and χ_2 correspond to the initial phase of ac dipole bumps 1 and 2, respectively. $\chi_1 - \chi_2 = \psi_0$ is the condition for exciting a single isolated resonance at $\nu_s = \nu_{\rm osc}$ with the spin flipper.

The ratio of the final polarization (P_f) to the initial polarization (P_i) after crossing a single spin resonance is given by the Froissart-Stora formula [12]:

$$\frac{P_f}{P_i} = 2\exp^{-(\pi/2)(|\epsilon|^2/\alpha)} - 1, \tag{5}$$

where ϵ is the resonance strength induced by the spin flipper, and the crossing speed (rate of sweep of $\nu_{\rm osc}$ through $\nu_s \approx \frac{1}{2}$) is

$$\alpha = \frac{\Delta\nu_{\rm osc}}{2\pi N}, \tag{6}$$

with $\Delta\nu_{\rm osc}$ being the ac dipole frequency span and N the number of turns of the sweep. To reach full spin flip, α has to be small enough or N large enough for beam particles to adiabatically follow the flip of the spin precession axis.

Spin tune spread reduction.—Besides eliminating the mirror resonance and any global vertical betatron oscillation driven by ac dipoles, the reduction of the spin tune spread is also critical for achieving full spin flip. The spin tune of a synchrotron with two Siberian snakes installed at opposite sides of the ring is given by

$$\nu_s = \frac{1}{2} + \frac{(1+G\gamma)(\theta_1-\theta_2)}{2\pi}, \tag{7}$$

where θ_1 and θ_2 are the integrated bending angles of the first half arc and second half arc, respectively. For the on-energy and on-axis protons, both θ_1 and θ_2 are equal (π) and the design-orbit spin tune is $\frac{1}{2}$, independent of the beam energy. This changes with synchrotron motion and the resulting momentum spread ($\Delta p/p$) [13]. The change in the bending angles are $\Delta\theta_1 = (x_1' - x_2')$ and $\Delta\theta_2 = (x_2' - x_1')$, respectively, where x_1' and x_2' are the slopes of the beam trajectory at the first and the second Siberian snake. The spin tune then becomes $\frac{1}{2} + (1+G\gamma)(x_2' - x_1')/\pi$. To the first order, x' can be expressed as $x' = D'(\Delta p/p)$, where D' is the slope of the dispersion function D, which measures orbit difference due to momentum offset, and $(\Delta p/p)$ is the momentum spread of beam particles. The momentum spread causes a spin tune spread when the dispersion slopes are different at the two Siberian snakes:

$$\Delta\nu_s = \frac{(1+G\gamma)}{\pi}(D_1' - D_2')\frac{\Delta p}{p}. \tag{8}$$

In the RHIC, this local dispersion slope difference between the two Siberian snakes is about 0.045 at 255 GeV, which corresponds to 0.007 spin tune spread for a beam with a momentum spread of 0.001. This is comparable to the proposed spin tune sweep range of 0.02. Hence, successful full spin flipping requires us to match the dispersion slopes. Since the $G\gamma$ values of 24 GeV ($G\gamma = 45.5$) and 255 GeV ($G\gamma = 487$) differ by a factor of 10, the required $\Delta D' = (D_1' - D_2')$ is 10 times smaller at 255 GeV than at 24 GeV to maintain the same spin tune spread $\Delta\nu_s$.

TABLE I. Parameters for the dc and ac dipoles at two different energies. The ac dipole strength is similar for the two energies, but the dc dipole strength and the induced resonance strength are different. ϕ_{osc} is given in units of radians.

Energy	$B\rho$	$B_{\mathrm{ac}}l$	ϕ_{osc}	$B_{\mathrm{dc}}L$	ψ_0	ϵ_k
24 GeV	79.4 Tm	0.01 Tm	0.005 86	0.89 Tm	29.9°	0.000 24
255 GeV	850 Tm	0.01 Tm	0.005 74	1.48 Tm	48.8°	0.000 57

The transition tune jump quadrupoles in the arcs were identified as effective elements for matching the dispersion slopes at the two Siberian snakes [14]. Four trim quadrupoles in each of the six RHIC arcs were adjusted so that the dispersion slope difference is very small and the distortion of β functions and tunes would be minimal [15].

Experimental results.—The spin flipper experiment was carried out at two different energies, injection at 24 GeV and store at 255 GeV. The 9 MHz rf cavity is the major rf system for beam operation both at injection and during acceleration. It was set to 22 kV at injection and 30 kV at store. A second "Landau" rf system ran at 197 MHz to maintain beam stability [16]. Its voltage was around 10 kV at injection and 15 kV at store. The bunch intensity was 1.5×10^{11} protons, with 111 bunches filled in one ring. The polarization was measured with the RHIC polarimeter [17].

The operation parameters of the spin flipper are listed in Table I. At injection, the beam can be refilled quickly, so that many experiments, such as flip efficiency with different $\Delta D'$ values, flip efficiency with different driving tune sweep speeds, were carried out at injection. Because of the larger beam size and larger orbit oscillation amplitude driven by the spin flipper at injection, the spin flipper could not be run at its full strength. With a local closed orbit bump of 26 mm, the spin flipper dc dipole current could be run at 900 A out of a maximum current of 1500 A.

Static measurements.—In static measurement, the polarization was measured as a function of the driving tune. The spin flipper was on for 3 sec, with the driving tune fixed then the polarization was measured. The measured polarization was the equilibrium polarization, which dropped when the driving tune was near the spin tune.

The spin tune spread is represented by the width of the polarization dip in Fig. 2. The polarization was completely lost when the driving tune was at the spin tune. The width of the polarization dip is related to the spin flipper resonance strength. The static model of the resonance width is also plotted for 24 and 255 GeV in Fig. 2. For the $\Delta D'$ suppressed lattice, the model width for 24 GeV matches well with the experimental data, while the measured width is wider than the static model for the 255 GeV case. This may indicate additional sources of spin tune spread at 255 GeV. At 24 GeV, the spin tune spread is greatly reduced, with the suppression of $\Delta D'$ declining from 0.074 to 0.003. This is a direct confirmation of the effect of $\Delta D'$ at the two Siberian snakes on the spin tune

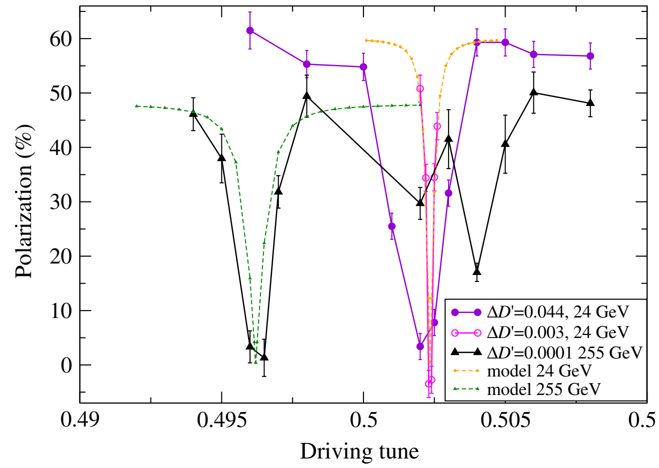

FIG. 2. The measured spin tune spectra for normal and $\Delta D'$ suppression lattices at 24 GeV and for a $\Delta D'$ suppression lattice at 255 GeV. At 24 GeV, spin tune $\nu_s \approx 0.502$ and the mirror resonance is at $1 - \nu_s \approx 0.498$. At 255 GeV, $\nu_s \approx 0.496$ and $1 - \nu_s \approx 0.504$. The difference in width between the two model resonance widths (dashed lines) is due to the different resonance strengths (see Table I).

spread. The good agreement between model, which has no spin tune spread, and experiment data for 24 GeV with the $\Delta D'$ suppression lattice indicates that, at least in this measurement, the spin tune spread is consistent with zero, which also puts a limit on any possible spin tune spread due to transverse orbital amplitude [18]. In addition, there is no polarization dip at $1 - \nu_s = 0.498$ for the large $\Delta D'$ case. This result at injection implies that the mirror resonance has been suppressed by this spin flipper design. The 255 GeV spectrum shows a polarization dip at the mirror resonance location, but it is not as deep as the primary resonance (near 0.496). The polarization loss at the mirror resonance implies that the local ac orbit bumps were not fully closed. As a result, the mirror resonance strength was weakened but the resonance was not completely eliminated.

Sweep measurements.—In a sweep measurement, the driving tune was swept for, typically, a 0.005 tune range over certain time (such as 1 sec). The polarization was measured before and after each sweep. At injection, the final to initial polarization ratio was measured with $\Delta D'$ as low as 0.003. The spin flipper was set to sweep from 0.4995 to 0.5045, and the spin tune was 0.5025. The final to initial polarization ratio was measured as a function of $\Delta D'$, and the results are shown in Fig. 3. The spin flipper sweep time was fixed at 3 sec during these measurements. It clearly demonstrates that the $\Delta D'$ suppression is critical to achieve high spin-flip efficiency. With a normal lattice where the $\Delta D'$ was large, the polarization was lost just with a single spin flipper sweep.

With the 0.005 tune sweep range and the given spin flipper strength, a 99% spin-flip efficiency is predicted for a sweep time of 0.6 sec or slower at 24 GeV from Eq. (5) and

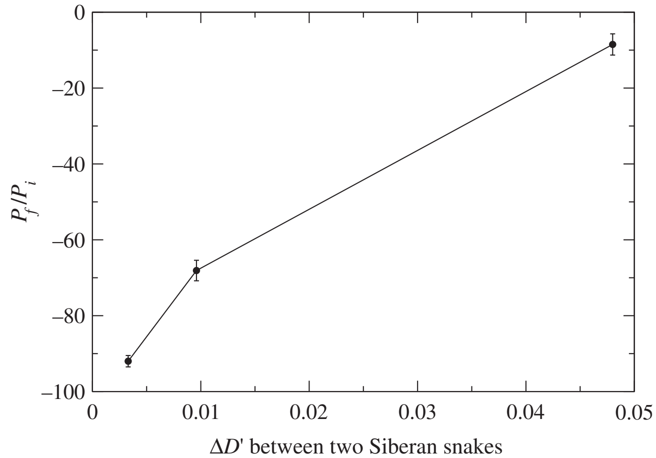

FIG. 3. The average final to initial polarization ratio for a 3 sec sweep time at injection as a function of $\Delta D'$ at the two Siberian snakes. The small $\Delta D'$ is critical for full spin flip.

numerical simulations [19]. The final to initial polarization ratio from Eq. (5) for the given spin flipper strength at injection is plotted in Fig. 4 as solid line. But this is an oversimplified model. In reality, the synchrotron motion and residual spin tune spread can have an impact on the final spin-flip efficiency. The measured spin-flip efficiencies for three different sweep times are also shown in Fig. 4. Each efficiency is the average of 10–12 spin flips. The best final to initial polarization ratio was obtained with a 1 sec sweep time: $-97.5 \pm 1.9\%$. This is close to the simple model prediction of -99%. At 0.5 sec, the final to initial polarization ratio is expected to be slightly worse due to a faster crossing speed, and the measured value $-95 \pm 2.6\%$ is indeed slightly smaller. For the slowest sweep time, 3 sec, the final to initial polarization ratio is only $-92.0 \pm 1.5\%$.

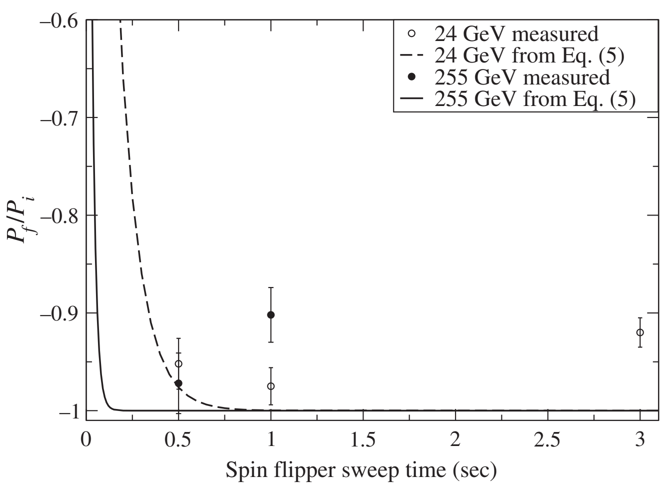

FIG. 4. The average final to initial polarization ratio at 24 and 255 GeV. The solid line is the polarization flip ratio from Eq. (5) for the resonance strength 0.000 24, and the filled points are the average spin-flip efficiencies for three different sweep times at 24 GeV. The dashed line and open points are for 255 GeV and the resonance strength 0.000 57.

There are several reasons for this. First, with a slower sweep speed, multiple spin resonance crossings with different resonance crossing speeds can happen due to synchrotron oscillation. This would result in a worse final to initial polarization ratio. Second, the polarization loss from weak higher order depolarizing resonances would be larger with a slower sweep speed.

With the smaller beam size at 255 GeV, the spin flipper can run at its full strength. The dc dipole current was 1500 A. At 255 GeV, the spin-flip efficiency was measured for three different $\Delta D'$ values. With a regular lattice where $\Delta D' = 0.045$, the polarization was completely lost with a single spin flipper sweep. With $\Delta D' = -0.003$, the final to initial polarization ratio was around $-36.7 \pm 6.6\%$. The above two measurements were done with a 3 sec sweep time. It is clear that further reduction of $\Delta D'$ is necessary. As at injection energy a faster sweep speed gave better spin-flip efficiency, the experiment at 255 GeV for $\Delta D' = 0.0001$ was carried out with a sweep time of 1 and 0.5 sec. With the 0.005 tune sweep range and the given spin flipper strength, the Froissart-Stora formula and numerical simulations predicted that a -99% final to initial polarization ratio could be reached with an optimum sweep time of 0.11 sec at 255 GeV. The final to initial polarization ratio from the given spin flipper strength at 255 GeV is plotted in Fig. 4 as a dashed line. The spin-flip efficiencies for the two different sweep times are also shown in Fig. 4. As before, each efficiency is the average of 10–12 spin flips. The better final to initial polarization ratio is at the 0.5 sec sweep time: $-97.2 \pm 3.1\%$. This is close to the simple model prediction of -99%. For the slower sweep time of 1 sec, the final to initial polarization ratio is $-90.2 \pm 2.8\%$. Similar to the 24 GeV case, the final to initial polarization ratio is worse with a slower sweep speed.

The spin flipper was also tested with a sweep time of 0.5 sec for a tune sweep ranging from 0.4935 to 0.5065. For this set of data, $\Delta D' = 0.0001$. This driving tune range covers primary resonance at the spin tune of 0.496, and its mirror resonance at 0.504. The final to initial polarization ratio was measured as $-100.8 \pm 9.8\%$. This is close to a full spin flip but with a large statistical error. Since the sweep range was 0.013 and the sweep time was 0.5 sec, the resonance crossing speed was faster. It seems that covering the mirror resonance may be fine. Since the orbit closure was adjusted just before this measurement, it is likely that the mirror resonance was indeed eliminated. More accurate measurements are needed to confirm this result.

Conclusions.—It has been shown that the nine-magnet spin flipper eliminated the mirror resonance. With the lattice for which the dispersion slope difference at the two Siberian snakes is greatly suppressed, a spin-flip efficiency of over 97% has been achieved for a polarized proton beam at 24 and 255 GeV in the presence of two full Siberian snakes. High spin-flip efficiency has been achieved by the nine-magnet spin flipper with the dispersion slope difference at the location of the two Siberian snakes as 0.003 at 24 GeV and 0.0001 at 255 GeV. Simulations are under way to quantify the sensitivity of spin-flip efficiency to the dispersion slope difference. The limited experimental data may indicate that a large driving tune sweep range covering the mirror resonance is possible. The spin-flip efficiency at 255 GeV could be further increased with a faster resonance crossing speed, either by a wider range or a shorter sweep time. These results demonstrate that the nine-magnet spin flipper will work for polarized proton experiments at the RHIC or a future electron ion collider.

The authors are thankful for the early work on the RHIC spin flipper by M. Bai. This work was supported by Brookhaven Science Associates, LLC, under Contract No. DE-AC02-98CH10886 with the U.S. Department of Energy.

[1] I. Alekseev *et al.*, Nucl. Instrum. Methods Phys. Res., Sect. A **499**, 392 (2003).
[2] A. Accardi *et al.*, Eur. Phys. J. A **52**, 268 (2016).
[3] Ya. S. Derbenev and A. M. Kondratenko, Part. Accel. **8**, 115 (1978).
[4] S. Y. Lee, *Spin Dynamics and Snakes in Synchrotrons* (World Scientific, Singapore, 1997).
[5] D. D. Caussyn *et al.*, Phys. Rev. Lett. **73**, 2857 (1994).
[6] B. B. Blinov *et al.*, Phys. Rev. Lett. **81**, 2906 (1998).
[7] B. B. Blinov *et al.*, Phys. Rev. Lett. **88**, 014801 (2001).
[8] M. A. Leonova *et al.*, Phys. Rev. Lett. **93**, 224801 (2004).
[9] M. Bai and T. Roser, Phys. Rev. ST Accel. Beams **11**, 091001 (2008).
[10] S. Mane, Phys. Rev. ST Accel. Beams **12**, 099001 (2009).
[11] M. Bai *et al.*, in *Proceedings of the International Particle Accelerator Conference (IPAC'10), Kyoto, Japan, 2010*, edited by A. Shirakawa and C. Petit-Jean-Genaz, p. 1224, http://accelconf.web.cern.ch/AccelConf/IPAC10/index.htm.
[12] M. Froissart and R. Stora, Nucl. Instrum. Methods **7**, 297 (1960).
[13] V. Ptitsyn *et al.*, in *Proceedings of the International Particle Accelerator Conference (IPAC'10), Kyoto, Japan, 2010*, edited by A. Shirakawa and C. Petit-Jean-Genaz, http://accelconf.web.cern.ch/AccelConf/IPAC10/index.htm.
[14] J. Kewisch *et al.*, BNL Collider-Accelerator Department Technical Note No. AP 478, 2013 (unpublished).
[15] C. Liu *et al.* (to be published).
[16] A. W. Chao, *Physics of Collective Beam Instabilities in High Energy Accelerators* (John Wiley, New York, 1993).
[17] H. Huang and K. Kurita, AIP Conf. Proc. **868**, 3 (2006).
[18] In this Letter, the focus is on spin tune spread due to beam energy spread.
[19] F. Méot *et al.*, BNL Collider-Accelerator Department Technical Note No. AP 589, 2017 (unpublished).